ARTICLE

A Single Switch High Gain Multilevel Boost Converter with Switched Inductor Topology for Photovoltaic Applications

Akkela Krishnaveni[1,3] and Rajender Boini*[2]

[1]Research Scholar, Dept. of EEE, Chaitanya (Deemed to be University), Warangal, Telangana, India.
[2]Professor, Dept. of EEE, Chaitanya (Deemed to be University), Warangal, Telangana, India.
[3]Lecturer, Department of Technical Education, Government of Telangana, India.

ABSTRACT

This paper proposes a new transformer-less single-switch high-gain dc-dc converter for solar power systems. The suggested converter is created by supplementing the conventional boost converter with a switched inductor cell plus a voltage multiplier stage. The converter has several benefits, including a high voltage conversion ratio, reduced voltage stress on semiconducting switches and diodes, a reduction in the need for gate drivers because only one switch is used, as well as constant input current to prolong the lifespan of the photovoltaic cell. The analytical waveforms of the recommended converter can be seen in the continuous conduction mode (CCM). The analysis of voltage stress is done. In the presence of parasitic components, increased voltage gain and efficiency were also obtained.The proposed high-gain converter topology is compared to recently published high-gain converter topologies in terms of performance. Using PSIM, a high-gain dc-dc converter's performance is studied and analysed with regard to its low switching voltage stress. The suggested converter is successful in stepping up 20V to 400V at 160W power capacity, while offering a continuous input source current at 95% efficiency.

*Corresponding author
Email Address: rajender_eee@chaitanya.edu.in
Date received: January 6, 2023
Date revised: January 4, 2024
Date accepted: January 5, 2024
DOI: https://doi.org/10.54645/202417SupDWR-69

INTRODUCTION

Technology is advancing quickly, which enhances the need for energy. Fossil fuels are a major source of electricity production almost anywhere in the world. However, a range of problems, including air pollution and additional environmental risks, have caused a decrease in the amount of fossil fuels used to produce power. The most commonly utilized renewable power source is solar energy because of its increased availability. However, there's a chance that partial shade conditions will result in less power being generated by PV. The utilization of energy from green sources in daily life is rapidly expanding. This is because the energy generated by green energy sources is clean and environmentally friendly. As of right now, renewable energy is the best available solution for environmental cleanup. Although nuclear energy can generate sustainable and ecologically friendly electricity, the process of post-processing it that is, containing radioactive waste is highly dangerous for habitats and will have long-term detrimental effects (Sutikno et al. 2022).

KEYWORDS

Boost Converter, Multilevel Boost Converter, High-Gain Converters, PV converters.

The main viable source of significant energy is energy from natural sources (RES), especially solar photovoltaic (PV) energy, which will soon totally replace energy generated from fossil fuel systems. DC-DC converters often come in two varieties: isolated or non-isolated. High-power applications are the primary use case for isolated DC-DC converters. However, the transformer's size rises with its presence. Initially, the voltage is increased using typical boost converters; however, this approach has a drawback because it places excessive stress from voltage over a switch, necessitating a high-rating switch. Conventional converters are frequently used to get around the problems of expense and poor conversion efficiency. For the necessary applications, a step-up chopper raises the small voltage level to a greater voltage level (Van Tan Nguyen et al. 2022; Goyal and Barai 2017).

However, because of a greater inrush current, its effectiveness is decreased. The system's switching frequency was increased to lessen the impact of inrush current, which puts a lot of strain on the switches. The gain restriction of boost-type converters is caused by both internal losses and stress over the switches. Additionally, it negatively impacts diodes, resulting in a decrease in their efficiency. For this reason, converters with linked inductance have been proposed as a fix (Mahmoudi et al. 2018; Meraj et al. 2020). Voltage spikes are produced by the leaking inductance when switches are off. Consequently, this results in reduced efficiency and elevated electromagnetic interference [EMI]. Active and passive clamping techniques can be applied to circumvent this. Therefore, the design of non-isolated boosting converters are presented (Mahar et al. 2019; Samadian et al. 2019) in order get the best of aforementioned issues. For PV applications, an interleaved high-gain step-up chopper was suggested in (Penghui et al. 2019). It has a high step-up gain and good efficiency, but because being having more components, the effect of parasitic part causes losses to grow at larger loads. Converters with switched capacitor topologies are used in (Priyadarshi et al. 2019; B. Wu et al. 2015) reports in order to attain a high DC gain. Although this method yields a large gain, the presence of impulsive current lowers the converter's stability. An automated output voltage- balancing non-isolated converter was described in (H. Kang and H. Cha 2018). A proposal for an active switched LC-network high gain step-up chopper was made in (Yuanwei et al. 2019). An inductor network and an active switching capacitor are used in this converter.

In (Rosas et al. 2010), a multiple boost converter that integrates a switching capacitor with the boost converter was described. With a high switching frequency and a steady input current, this converter functions. Additionally covered is the cascaded architecture for n-stage conversion. In (Shahir et al. 2018), a voltage-lift technique-based step-up chopper with just one switch is described. The inductor and capacitor two energy-storage components are the foundation of this method. However, the system becomes more complex like the quantity of components rises. In (Ismail et al. 2008), a novel class of 3-diode, 1-switch, PWM DC-DC converters working at constant duty ratio and frequency was covered. The diodes are under less voltage stress, and conduction losses are reduced. Its voltage gain can be raised by integrating voltage multipliers. There have been also reports of a one switch quadratic buck-boost converter. These single-switch converters all have a greater quantity of diodes, capacitors, and transformers. The converter described in (Nagaraju and Rajender 2023) makes use of two switches and the switched inductor concept. The quasi-switched converter, which generates high voltages with a low duty ratio, is described in (X. Hu et al. 2020). A study of an interleaved converter with inverting capabilities may be found in (Meraj et al. 2021) despite the high gain, more components are needed overall. To increase the dc-link voltage, a high-gain transformer-less converter with fewer components is therefore required. Nevertheless, there could be a number of drawbacks, including more complexity, lower dependability, and higher expenses. Furthermore, in high-gain applications, the diode recovery problem is a significant problem (Alghaythi et al. 2020; Mirzaee et al. 2020). Additionally, isolated boost converters may be used with a transformer to demonstrate bigger voltage gains. However, the leaking inductance will cause a number of issues, including EMI. Transformer losses will simultaneously result in elevated costs, inefficient performance and more intricate control techniques (Alghaythi et al. 2020; Yuttana et al. 2017). The step-up choppers fly-back combo topology is made to achieve high DC gain. Comparing this design to other converters now on the market, it is conceivably easy. However, it takes time to keep the capacitors' voltage balanced (Nagaraju and Rajender 2023). The reverse recovery losses of the diode have a big impact on the converter's effectiveness. When the boost converter runs on a discontinuity current model or in critical current mode, the converse recovery loss can be reduced (Mohseni et al. 2018). As a result, there will be more input current stress and current ripples. This must be defeated by the use of a large filter. As a result, it is inappropriate for high-power uses (Maalandish et al. 2018). Low thermal stress delivery can be achieved by using Interleaved Boost Converters (IBC) to increase both power level and density. Because of this, it displays reduced ripple current at duty cycle ratios of less than 0.5 (Ranganathan and Arun Noyal 2021; Sathiya et al. 2021). In contrast, it has some disadvantages when used in a PV-grid-linked system. Low efficiency results from the high voltage stress across the IGBT. A non-isolated capacitor with a diode is developed in order to obtain a greater gain (Maalandish et al. 2018). VM units expanded to "n" steps in order to achieve this. By raising the duty cycle and VM units, the level can be raised. As a result, its efficiency is roughly 93.6%. A new triple mode has been created (Bhaskar et al. 2020)~~,~~; however, for the purpose of achieving better voltage gain, more components are needed. Its efficiency in real-world use is around 93.86% at 500 W. Interleaved MBC using VM cells is a unique converter that is designed. At approximately 300W of load power, its efficiency stands at 93.56%. This circuit has a large loss because of the diodes. Given that quasi-Z-source converters have an unchanged current supply, there is relatively little stress on the switches and capacitors. However, they don't show a lot of increase (Padmavathi and Natarajan 2020; Meinagh et al. 2020).

It is decided to create a converter with more gain and less switch stress. At 66 W, its efficiency is approximately 93.6%. With a lower duty ratio, this converter shows strong gain. With a duty ratio of 0.6, it achieves its maximum gain over 12 times the optimal conditions. However, in actuality, it is dependent on load and parasitic component values (Ahmad et al. 2020). Effectiveness in both the step-up/down modes is 89% and 91.2%, respectively, which is comparable. 93.9 is the highest efficiency when operating in boost mode with an output current equal to 0.6 A (Saravanan and Babu 2018). In (Sarikhani et al. 2021It is suggested to use a unique converter having a steady input current. Nevertheless, the voltage transfer ratio is limited at large duty ratios. To improve cross-regulation and efficiency, a single-stage AC/DC FLC with three output windings and a synchronous rectification (SR) function is employed (Chung-Ming and Huang-Jen 2021). With a maximum efficiency of 87%, it outperforms a conventional Schottky diode by about 3%. Theoretically, this converter shows significant gains. There is a noticeable reversal voltage across the switches whenever blocking voltage arises. Its leaking inductance's stored energy is the cause. Dampening circuits are therefore required, which raises expenses and lowers efficiency. To attain extreme voltage conversion ratio, a coupled inductor (CI) and voltage multiplier

(VM) are utilized without a high-duty cycle. In order to reduce transmission losses and boost effectiveness in switches, it is advised to utilise a switch that has little $Rds_{(on)}$ (Hasanpour et al. 2020). This paper suggests a flyback-forward-high-gain chopper with zero current switching. By providing soft switching conditions with an auxiliary circuit in place of extra switches, the efficiency is raised (Jahangiri et al. 2020). Power electronics are crucial for obtaining the most energy possible from clean and renewable energy sources. A proposed schematic system is shown in Figure 1. High DC voltage-gain choppers are used in series between the source of electricity and the device being utilized to convert low DC voltage (between 12 and 60 volts) from fuel cells, PV (photovoltaic) solar panels, and batteries to high DC voltage (between 200 and 300 volts).

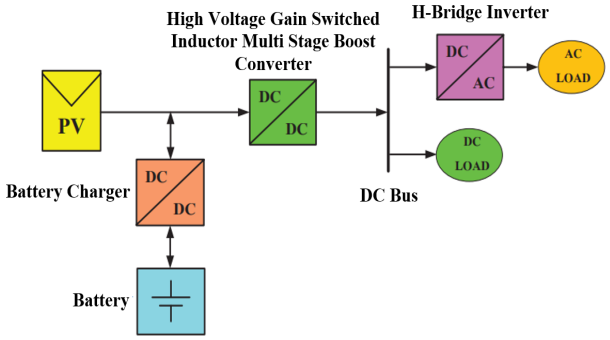

Figure 1: Simple schematic of the proposed system

This work implements a new transformer-less high-gain direct current converter that increases voltage using a VMC. The proposed topology's appealing qualities include high gain during a reduced duty ratio. There is reduced potential stress in the converter. The converter operates simply since it just uses one gate signal for a single switch. The architecture can be used for PV applications because its input current is constant. The suggested topology's structure is covered in Section 2, along with a thorough ideal analysis, while Section 3 examines the steady-state analysis. In Section 4, a comparative analysis of the suggested converter with several converters that are similar is made. Section 5 presents the modelling and experimental results, as well as the comparison and evaluation of alternative converters

PROPOSED CONVERTER DESIGN AND OPERATING MODES

This paper introduces a high DC voltage gain chopper with one power switch, i.e., an IGBT, six no. of diodes, three no. of inductors, and two no. of capacitors. Figure 2 shows the suggested converter topology. The converter functions in two switching modes because there is only one switch. i.e, IGBT Switch ON mode and IGBT Switch OFF mode. There is a wide variety of resistive loads in the suggested converter driving capabilities and operates in CCM.

Power switch on mode

When IGBT is making the diodes activate, power diodes D1, D2, and D4 are forward biased and start conducting, and power diodes D3, D5, and D6 are off and do not conduct because of the reverse polarity across them. Due to the supply voltage, a linear current flow through the inductors L1 and L2, hence the energy that is held on them until their polarity reaches the supply voltage. In this Mode, voltage polarities and current directions are shown in figure 3. Following the brief transient period, due to the current I_{L3} flowing through the capacitor C1 and inductor L3 the capacitor C1 magnetises inductor L3 in the direction shown in figure 3. IGBT switch current is the algebraic sum of input current I_{In} and inductor L3 current I_{L3}. The capacitor C2 supplies the required load current.

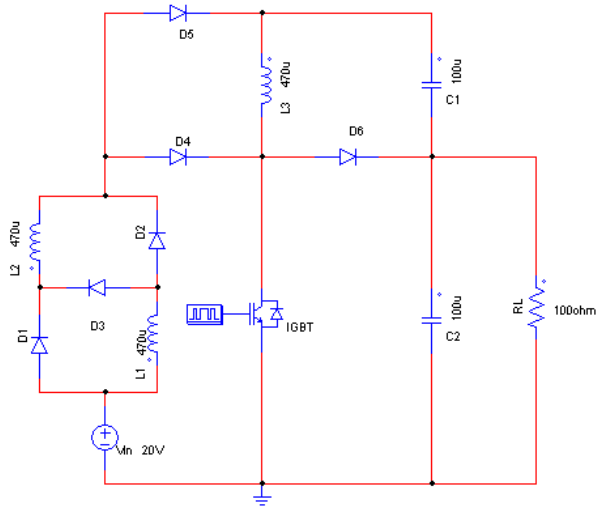

Figure 2: Suggested converter topology

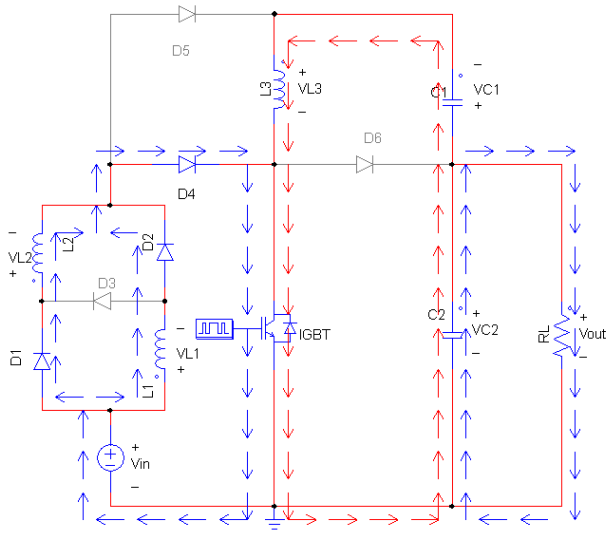

Figure 3: IGBT switch ON Mode: voltage polarities and current directions

The applied DC voltage V_{IN} is equivalent to the voltage that appeared at the magnetising elements L1 and L2, $V_{L1(on)}$ and $V_{L2(on)}$.

$$V_{L1(ON)} = V_{in} \quad \ldots (1)$$

The voltage that appeared at inductor L3, $V_{L3(ON)}$, is the same as the voltage across C1, V_{C1}. Hence,

$$V_{L3(ON)} = V_{out} + V_{C1} \quad \ldots (2)$$

Power switch off mode

To keep the current flowing in the same direction as when IGBT is activated, the polarity of the inductors L1, L2, and L3 is reversed. Figure 4 shows that, the diodes D3, D5, and D6 are on in this mode, whereas D1, D2, and D4 are erroneous since they have the opposite bias polarity across them. The energy that was previously held in L1, L2, and L3 is now freed and released to C1 and C2. Using the polarity illustrated in Figure 4, the capacitor C2 begins to charge and develops a voltage across the capacitor VC2 same as Vout. When operating in this mode, Inductors VL1(OFF) and VL2(OFF) have voltages across them that equal the variation between Vin and VOUT, and the

capacitor C1 voltage VC1. Further, the inductor L3 voltage VL3(OFF) is equal to the voltage across capacitance C1.
Those relationships are depicted as follows:

$$V_{L1(OFF)} + V_{L2(OFF)} = V_{in} - V_{C1} - V_{out} \quad \ldots.(3)$$

$$V_{L3(OFF)} = V_{C1} \quad \ldots(4)$$

Consider both L1 and L2 are identical values; both inductors have the same voltage.

$$V_{L1(OFF)} = \frac{(V_{in} - V_{C1} - V_{out})}{2} \quad \ldots.(5)$$

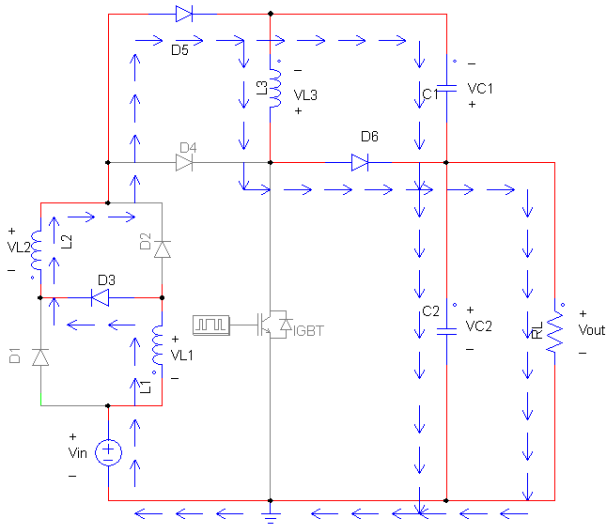

Figure 4: IGBT switch OFF Mode: voltage polarities and current directions

STEADY-STATE ANALYSIS

Even when substantially loaded, the proposed converter continues to operate in CCM mode. The evaluation regarding a DC voltage gain, IGBT's voltage stresses, and efficiency is described in the following text, presuming that the recommended converter works in CCM mode and that every component utilized in the implementation is ideal.

DC voltage gain

Volt-second balance is applied to the inductor L1 in both on and off modes, using the equations (1) and (5) and duty cycle Dy.

$$V_{in} \times Dy = \frac{(V_{C1} + V_{out} - V_{in})}{2} \times (1 - Dy) \quad \ldots.(6)$$

$$V_{in}(2Dy + 1 - Dy) = (V_{C1} + V_{out}) \times (1 - Dy) \quad \ldots(7)$$

$$V_{in}(1 + Dy) = (V_{C1} + V_{out}) \times (1 - Dy) \quad \ldots.(8)$$

$$(V_{C1} + V_{out}) = \frac{V_{in}(1 + Dy)}{(1 - Dy)} \quad \ldots(9)$$

Utilizing equations (2) and (4) for L3 and applying the volt-second balance results in

$$(V_{out} + V_{C1}) \times Dy = -V_{C1} \times (1 - Dy) \quad \ldots(10)$$

$$-V_{out} \times Dy = V_{C1} \quad \ldots(11)$$

By Adding V_{out} in both sides we will get

$$V_{out} - V_{out} \times Dy = V_{out} + V_{C1} \quad \ldots(12)$$

By equating equation (9) and equation (12), we get

$$V_{out} \times (1 - Dy) = \frac{V_{in}(1 + Dy)}{(1 - Dy)} \quad \ldots(13)$$

$$V_{out} = \frac{V_{in}(1 + Dy)}{(1 - Dy)^2} \quad \ldots(14)$$

There four voltage gain G is equal to

$$\frac{V_{out}}{V_{in}} = \frac{(1 + Dy)}{(1 - Dy)^2} \quad \ldots(15)$$

The suggested high-gain chopper DC voltage boost transfer function in steady-state is presented in (13), demonstrates that the output voltage has an inverse relationship to the $(1 - Dy)^2$. As a result, raising the duty ratio in (15) raises the output voltage quadratically.

Voltage stresses

The diode D6 turns on when the IGBT is in switch-off mode, and the switch itself aligns itself with the load. As a result, switch voltage is equals V_{out}.

$$V_{S1(OFF)} = V_{out} = \frac{V_{in}(1 + Dy)}{(1 - Dy)^2} \quad \ldots(16)$$

During switch-on mode, the diodes D1 and D2 are off. From figure 3, it can be observed that the D1and D2 voltages equal to the L1 and L2 voltages, respectively.

$$V_{D1(OFF)} = V_{L1(OFF)} = L_1 \times \frac{\Delta I_{L1}}{(1 - Dy).T} \quad \ldots(17)$$

$$V_{D1(OFF)} = V_{L1(OFF)} = L_1 \times \frac{\Delta I_{L1}}{(1 - Dy)} \times f_s \quad \ldots(18)$$

and

$$V_{D2(OFF)} = V_{L2(OFF)} = L_2 \times \frac{\Delta I_{L2}}{(1 - Dy).T} \quad \ldots(19)$$

$$V_{D2(OFF)} = V_{L2(OFF)} = L_2 \times \frac{\Delta I_{L2}}{(1 - Dy)} \times f_s \quad \ldots(20)$$

Where f_s is switching frequency

During switch-off mode, the diodes D3 is off. From figure 2, It is evident that the voltage tension between diodes D3 is equal to the voltage across inductors L1 or L2.

$$V_{D3(OFF)} = V_{L1(ON)} = L_1 \times \frac{\Delta I_{L1}}{Dy.T} \quad \ldots(21)$$

$$V_{D3(OFF)} = V_{L1(ON)} = L_1 \times \frac{\Delta I_{L1}}{Dy} \times f_s \quad \ldots(22)$$

When D4 is off, the voltage stress across D4 can be found by KVL around the loop, which contains D4, V_{in}, V_{out}, L1, and L2. This gives

$$V_{D4(OFF)} = V_{in} - V_{out} + V_{L1} + V_{L2} \quad \ldots(23)$$

$$V_{D4(OFF)} = V_{out} \times \frac{(2Dy - Dy^2)}{(1 + Dy)} + V_{L1} + V_{L2} \quad \ldots(24)$$

The voltage stress across D5 can be calculated in switch-on mode. From figure 2, it can be observed that it is equal to the inductor L3 voltage.

$$V_{D5(OFF)} = V_{L3(ON)} = L_3 \times \frac{\Delta I_{L3}}{Dy.T} \quad \ldots(25)$$

$$V_{D5(OFF)} = V_{L3(ON)} = L_3 \times \frac{\Delta I_{L3}}{Dy} \times f_s \quad \ldots(26)$$

KVL applied to the loop contains D6, Switch, and capacitor C2, i.e., output voltage $V_{out,}$ can be used to compute the voltage stress across D6. Hence,

$$V_{D6(OFF)} = V_{out} = V_{in}\left(\frac{1+Dy}{(1-Dy)^2}\right) \quad \ldots(27)$$

EFFICIENCY ANALYSIS

The overall power loss in IGBT is the sum of the static and dynamic losses. When an IGBT is turned on, the channel resistance causes a loss of static power; however, when the device is switched, the channel resistance causes a loss of dynamic power. The equation that can be utilized to determine an IGBT's static power loss is

$$P_{IGBT} = I^2{}_{S(rms)} \times r_{Ds(on)} \quad \ldots(28)$$

Where, $r_{Ds(on)}$ denotes the IGBT's on-state resistance and $I_{S(rms)}$ denotes the rms current flowing through it.

$$P_{IGBT,dynamic} = \frac{V_{in} \cdot I_{out}}{3} \quad \ldots(29)$$

As a result, the switch's overall power loss is indicated by

$$P_{IGBT,static} = I^2{}_{S(rms)} \times r_{Ds(on)} + \frac{V_{in} \times I_{out}}{3} \quad \ldots(30)$$

A diode's total power loss which consists of the power loses due to diodes on-state resistance during forward bias. Following that, a diode's power loss can be expressed as follows:

$$P_D = V_F \times I_{D(avg)} + I^2{}_{D(rms)} \times r_D \quad \ldots(31)$$

In equation (31), V_F stands for the diode's forward voltage drop, r_D for its forward junction resistance, and $I_{D(rms)}$ for the typical amount of current flowing via the diode once it is activated.

$$P_C = I^2{}_{C(rms)} \times ESR \quad \ldots(32)$$

The "equivalent series resistance" (ESR) and the "rms value of capacitor current" I_(C(rms)) are used in equation (32). In a similar manner, The approach that follows can be used to calculate an inductor's power loss:

$$P_L = I^2{}_{L(rms)} \times r_{series} \quad \ldots(33)$$

In equation (33), the current passing through the inductor's root mean square value $I_{L(rms)}$, and r_{series} is the series resistance of the substance that the inductor is manufactured from. Consequently, In the recommended converter architecture, the total power loss will be:

$$P_{loss(to)} = P_{IGBT} + 6P_D + 2P_{L1} + P_{L3} + P_{C1} + P_2 \quad \ldots(34)$$

Using these losses, efficiency can be expressed as

$$\eta = \frac{P_{out}}{P_{out} + P_{loss(total)}} \quad \ldots(35)$$

PASSIVE COMPONENTS' DESIGN

No matter what topology is employed, selecting the parameters of the energy-storing element was based on a crucial aspect of how high-gain choppers behave and work. The consistency and regulation of the resultant DC voltage levels are influenced by the degree of tolerance in the current ripple of inductive devices and the voltage that ripples in capacitors. Generally speaking, the largest ripple over the current or voltage flowing through an inductor or capacitor shouldn't be greater than 10% of the maximum current or voltage that would flow through it. These suppositions provide a rational guideline for figuring out how many inductors as well as capacitors are needed for an efficient design that generates a steady flow of current and maintains an even level of voltage across the load being utilised. The equations employed to ascertain the nominal values for the inductors and capacitors used in this recommended boost converter keep this principle in mind.

Design of inductor L1

Consider identical inductors L1 and L2, which are equal to L. Then, in order to calculate the voltage that exists across an inductor using the equation

$$V_{in} = (L1 + L2)\frac{dI_{L1}}{dt} \quad \ldots.(36)$$

$$V_{in} = \frac{L}{2}\frac{dI_{L1}}{dt} \quad \ldots.(37)$$

Consequently, the current flowing via inductor L1 is represented by

$$\Delta I_{L1} = \frac{2\,V_{in}\,Dy\,T}{L_1} \quad \ldots.(38)$$

Similarly, the current flowing via inductors L2 and L3 is given as

$$\Delta I_{L2} = \frac{2\,V_{in}\,Dy\,T}{L_2} \quad \ldots.(39)$$

$$\Delta I_{L3} = \frac{V_{C1}\,Dy\,T}{L_3} \quad \ldots.(40)$$

The formula for the amount of voltage over the first capacitor, C1, is

$$V_{C1} = V_{in}\left(\frac{1}{1-Dy}\right) \quad \ldots(41)$$

Or,

$$V_{C1} \times Dy = V_{in}\left(\frac{Dy}{1-Dy}\right) \quad \ldots(42)$$

Or,

$$\frac{V_{C1}\,Dy\,T}{L_3} = V_{in}\left(\frac{Dy}{1-Dy}\right).\ \frac{T}{L_3} \quad \ldots.(43)$$

Equating (39) and (40),

$$\Delta I_{L3} = V_{in} \times \frac{Dy}{(1-Dy) \times f_s \times L_3} \quad \ldots.(44)$$

Rewriting Equation (38) for L1

$$L_1 = \frac{2\,V_{in}\,Dy\,T}{\Delta I_{L1}} \quad \ldots(45)$$

L1 or L2 in terms of output voltage and switching frequency

$$L_1 \text{ or } L_2 = 2V_{out} \frac{(1-Dy)^2}{1+Dy} \times \frac{Dy\,T}{\Delta I_{L1}} \quad \ldots(46)$$

The relationship shown in (46) provides the smallest possible value for both L1 and L2 inductors that may be employed. The IGBT switching frequency is f_s, the voltage that comes from the converter in DC form is V_{out}, and the duty cycle is Dy. The ΔI_{L1} and ΔI_{L2} are the ripples that occur in both the L1 and L2 inductors current.

Design of inductor L3

Rewriting Equation (44) for L3:

$$L_3 = \frac{V_{in} \times Dy}{(1-Dy) \times f_s \times L_3 \times \Delta I_{L3}} \quad \ldots.(47)$$

L3 in terms of output voltage and f_s,

$$L_3 = \frac{V_{out} \times Dy \times (1+Dy)}{(1+Dy) \times f_s \times L_3 \times \Delta I_{L3}} \quad \ldots.(48)$$

In terms of V_{in} or V_{out}, respectively, (47) and (48) provide the minimal L3 inductor value that is needed, with ΔI_{L2} denoting the ripple degree of L3 current.

Design of capacitor C1

L3 and C1 are connected in series in power switch ON mode, and the electrical current passing via this particular branch is represented as follows:

$$I_{C1} = C_1 \times \frac{\Delta V_{C1}}{\Delta t} \quad \ldots.(49)$$

The version of equation (49) above is as follows when Switch ON Mode is engaged:

$$C_1 = I_0 \times \frac{Dy\,.T}{\Delta V_{IN}} \quad \ldots.(50)$$

From equation (41) Submitting Vin in equation (50), we will get

$$C_1 = \frac{I_0\,.Dy\,.T}{V_{C1}(1-Dy)} \quad \ldots.(51)$$

Equation (51) in terms of switching frequency is,

$$C_1 = \frac{I_0\,.Dy}{V_{C1} \times (1-Dy) \times f_s} \quad \ldots.(52)$$

The equation in (52) provides the smallest value of C1 that can be employed with ΔV_{C1} voltage ripples over C1.

Design of capacitor C2

The flow of current via capacitor C2 gets supplied from the following equation

$$I_{C2} = C_2 \times \frac{\Delta V_{C2}}{\Delta t} \quad \ldots.(53)$$

From the above equation C2 is:

$$C_2 = I_{C2} \times \frac{Dy}{\Delta V_{out} \times f_s} \quad \ldots.(54)$$

The equation in (54) provides the smallest value of C2 that can be employed with ΔV_{C2} voltage ripples over C2.

RESULTS AND DISCUSSION

Table 1 displays the converter's specifications. Figure 5 shows the PSIM implementation diagram for the suggested converter. It consists of three inductors of 470 µH, ESR = 0.2 Ω, two capacitors of rating C1, C2 = 100 µF 250 V, ESR = 0.15 Ω, and six diodes. When a 20V DC input voltage is given to the proposed converter, it can boost the voltage up to 400 volts with a duty ratio of 0.63. Its input and output voltages and currents are shown in figures 6 and 7. Figure 8 shows the inductor L3 current wave form. It is evident from figures 6 and 7 that the suggested converter has a gain of 20, i.e., 400/20, at a duty ratio of 0.63.

Table 1: Ratings of converter components

Components	Ratings
Input Voltage V_{in}	20V
R load	1000 Ω
Switching frequency f_s	25KHz
Inductors	L1 = L2 = L3 = 470 µH, ESR = 0.2 Ω
Capacitors	C1 = C2 = 100 µF 250 V, ESR = 0.15 Ω
D1, D2, D3, D4, D5 and D6	SF8L60USM
Gate Drivers IC	TLP250H

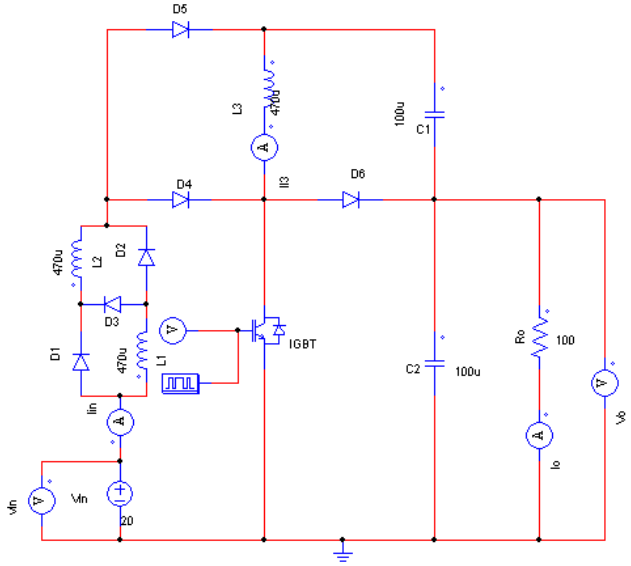

Figure 5: PSIM implementation diagram for the suggested converter

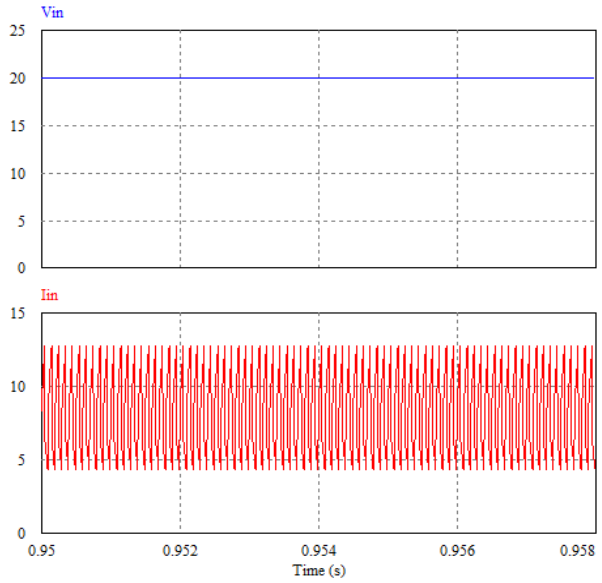

Figure 6: Converters input voltage and current wave form.

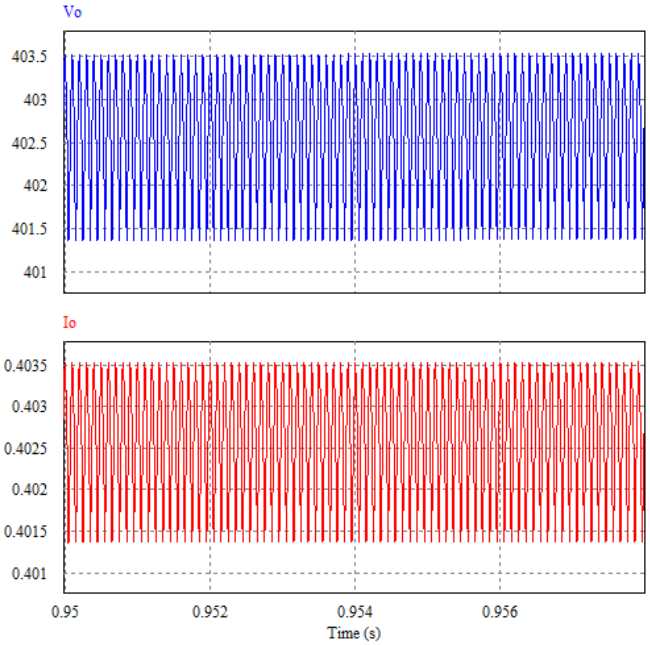

Figure 7: Converters output voltage and currents wave forms

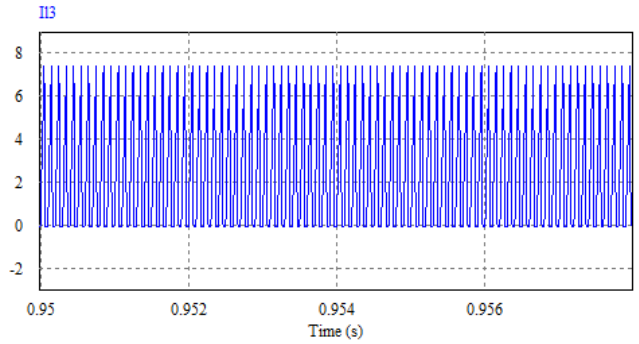

Figure 8: Inductor L3 current wave form.

COMPARISON AND EVALUATION OF ALTERNATIVE CONVERTERS

In this segment, the increased DC voltage gain converters discussed in the study are contrasted. Comparing similar recently suggested converters is shown in Table 2.

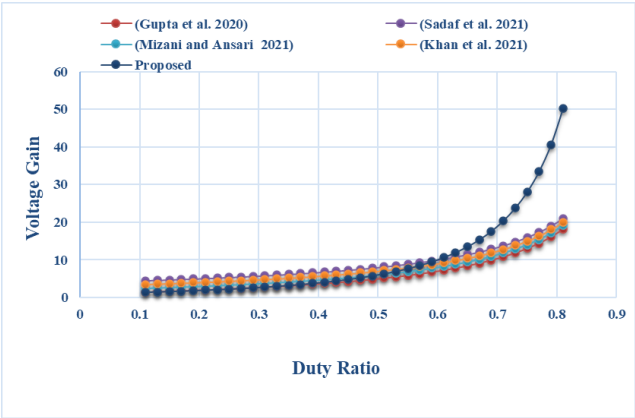

Figure 9: Comparison of voltage gains of different converters

Two switches, nine diodes, four inductors, and one capacitor formed the converter suggested in (Gupta et al. 2020) but it has a gain of only 7.8. The converter suggested in (Sadaf et al. 2021) utilizes same number of components, but it has a gain of 10 only at a duty cycle of 0.63. The converter proposed by (Mizani and Ansari 2021) has a gain of 8.8 only Utilizing 16 no. of components. In (Khan et al. 2021) same number of components was utilized to achieve a gain of 9.8 at 0.63 duty cycle. In the proposed converter, we utilized only 12 components and achieved a gain of 12. It achieved high gain by utilizing fewer components. It has additionally had fewer voltage stresses and continuous input current. Figure 9 shows that the duty cycle vs voltage gain graph. The suggested converter achieves a quadratic gain, and after 0.6 duty cycle, it has achieved a very high gain relative to the alternative converters proposed in table 2.

Table 2: Analysis of component counts and voltage improvements across various topologies

Topology Presented in	No. of Switches and Diodes	No. of Inductors and Capacitors	Total No. of Components	Voltage Gain ($\frac{V_{out}}{V_{in}}$)	Voltage Stress at switches ($\frac{V_{sw}}{V_{in}}$)
(Gupta et al. 2020)	2+9	4+1	16	$\frac{1+3Dy}{1-Dy}$	$\frac{1+3Dy}{1-Dy}$
(Sadaf et al. 2021)	2+4	2+4	12	$\frac{4}{(1-Dy)}$	$\frac{1}{2}$
(Mizani and Ansari 2021)	1+5	3+7	16	$\frac{2+2Dy}{1-Dy}$	$\frac{1}{(1-Dy)}$
(Khan et al. 2021)	2+7	4+3	16	$\frac{5+Dy}{(1-Dy)}$	$S1 = \frac{5+Dy}{(1-Dy)}$ $S2= \frac{1}{(1-Dy)} * \frac{1}{(1-Dy)}$
Proposed converter in this paper	1+6	3+2	12	$\frac{1+Dy}{(1-Dy)^2}$	$\frac{1+Dy}{(1-Dy)^2}$

CONCLUSION

In contrast to some recent proposals for high-voltage DC gain boost converters, a novel DC-DC surge converter with a reduced number of elements is provided in this study. For the direct current (DC) gain, potential stresses, and efficiency of the suggested boost converter, simulations were conducted. The simulation findings validated the an effectively developed design. The comparison made it clear that the design

recommended successfully achieved high voltage gain as its objective in minimizing the component count.

CONFLICT OF INTEREST

The authors declare that there is no conflict of interest.

REFERENCES

A. Priyadarshi, P. K. Kar, and S. B. Karanki, "Switched capacitor based high gain DC-DC converter topology for multiple voltage conversion ratios with reduced output impedance," Journal of Power Electronics, 2019, vol. 19, pp. 676–690.

Ahmad J, Lin CH, Zaid M, Sarwar A, Ahmad S, Sharaf M, et al. A new high voltage gain DC to DC converter with low voltage stress for energy storage system application. Electronics. 2020, 9(12):2067.

Alghaythi ML, O'Connell RM, Islam NE, Khan MMS, Guerrero JM. A high step-up interleaved DC-DC converter with voltage multiplier and coupled inductors for renewable energy systems. IEEE Access.2020; 8:123165–123174.

Alghaythi ML, Oconnell RM, Islam NE, Guerrero JM. A Non-Isolated High Step-Up Interleaved DC-DC Converter with Diode-Capacitor Multiplier Cells and Dual Coupled Inductors. In 2020 52nd North American Power Symposium (NAPS), 2020, 1–6.

B. Wu, S. Li, K. Smedley, and S. Singer, A family of two-switch boosting switched-capacitor converters, IEEE Transactions on Power Electronics, 2015, vol. 30, pp. 5413–5424.

Bhaskar MS, Almakhles DJ, Padmanaban S, Holm-Nielsen JB, Kumar AR, Masebinu SO. Triple-mode active-passive parallel intermediate links converter with high voltage gain and flexibility in selection of duty cycles. IEEE Access.2020, 8:134716–134727.

Chung-Ming L, Huang-Jen C. Three-output flyback converter with synchronous rectification for improving cross-regulation and efficiency. Electronics. 2021, 10(4), 430.
doi: 10.1109/ACCESS.2021.3077055.
doi: 10.1109/TPEC51183.2021.9384956.

E. H. Ismail, M. A. Al-Saffar, A. J. Sabzali, and A. A. Fardoun, A family of single-switch PWM converters with high step-up conversion ratio, IEEE Transactions on Circuits and Systems I: Regular Papers, 2008, vol. 55, pp. 1159–1171.

F. M. Shahir, E. Babaei, and M. F. Farzad, Voltage-lift technique based non-isolated boost DC–DC converter: analysis and design, IEEE Transactions on Power Electronics, 2018, vol. 33, pp. 5917–5926.

G. Yuanwei, Y. Chen, B. Zhang, D. Qiu, and F. Xie, "High step-up DC-DC converter with active switched LC-Network for photovoltaic systems," IEEE Transactions on Energy Conversion, 2019, vol. 34, no. 1, pp. 321–329.

Goyal S, Barai M. Design and implementation of high gain boost converter with voltage-mode control. In 2017 IEEE International Conference on Power, Control, Signals and Instrumentation Engineering (ICPCSI), 2022, 1850–1855.

Gupta, N.; Bhaskar, M.S.; Almakhles, D.; Sanjeevikumar, P.; Subramaniam, U.; Leonowicz, Z and Mitolo, M. (2020). Novel non-isolated quad-switched inductor double-switch converter for DC microgrid application. Proceedings of the 2020 IEEE International Conference on Environment and Electrical Engineering and IEEE Industrial and Commercial Power Systems Europe (EEEIC / IandCPS Europe), Madrid, Spain,2020, 1-6.

H. Kang and H. Cha, "A new non isolated high-voltage-gain boost converter with inherent output voltage balancing," IEEE Transactions on Industrial Electronics, 2018, vol. 65, pp. 2189–2198.

Hasanpour S, Siwakoti Y, Blaabjerg F. New single-switch quadratic boost DC/DC converter with low voltage stress for renewable energy applications. IET Power Electronics.2020, 13(19):4592–4600. https://doi.org/10.1049/pel2.12007.
https://doi.org/10.1093/ce/zkac037
https://doi.org/10.12913/22998624/161447

J. C. Rosas-Caro, J. M. Ramirez, F. Z. Peng, and A. Valderrabano, "A DC–DC multilevel boost converter," IET Power Electronics, 2010, vol. 3, no. 1, pp. 129–137.

Jahangiri S, Delshad M, Vesali M. A new single-switch ZCS flyback-forward converter with high power density. IETE Journal of Research.,2020, 68, 3428–3438.

M. Meraj, M. S. Bhaskar, B. P. Reddy, and A. Iqbal, "Non-isolated DC–DC power converter with high gain and inverting capability," IEEE Access, 2021, vol. 9, pp. 62084–62092.

Maalandish M, Hosseini SH, Ghasemzadeh S, Babaei E, Jalilzadeh T. A novel multi-phase high stepup DC/DC boost converter with lower losses on semiconductors. IEEE J. Emerg. Sel. Top. Power Electron.2018, 7(1):541–554.

Maalandish M, Hosseini SH, Jalilzadeh T. High step-up DC/DC converter using switch-capacitor techniques and lower losses for renewable energy applications. IET Power Electronics.2018, 11 (10):1718–1729.

Mahar AM, Shaikh PH, Mahar AR, Memon ZA, Khatri SA, Shah SF. Simulation of efficient non-isolated DC-DC boost converter topology for photovoltaic application. In AIP Conference Proceedings. 2019, 2119(1):020019.

Mahmoudi M, Ajami A, Babaei E. A non-isolated high step-up DC-DC converter with integrated 3 winding coupled inductor and reduced switch voltage stress. International Journal of Circuit Theory and Applications. 2018, 46(10):1879–1898.

Meinagh AA, Yuan FJ, Yang Y. Analysis and design of a high voltage-gain quasi-Z-source DC-DC converter. IET Power Electron. 2020, 13:1837–1847.

Meraj M, Bhaskar MS, Iqbal A, Al-Emadi N, Rahman S. Interleaved multilevel boost converter with minimal voltage multiplier components for high-voltage step-up applications. IEEE Trans. Power Electron.2020, 35:12816–12833.

Mirzaee A, Moghani JS. Coupled Inductor-Based High Voltage Gain DC–DC Converter for Renewable Energy Applications. IEEE Transactions on Power Electronics. 2020; 35(7):7045–7057.

Mizani A; Ansari S A; Shoulaie A; Davidson JN; and Foster MP. Single-active switch high-voltage gain DC–DC converter

using a non-coupled inductor. IET Power Electron.2021, 14:492–502.

Mohseni P, Hosseini SH, Sabahi M, Jalilzadeh T, Maalandish M. A new high step-up multi-input multioutput DC-DC converter. IEEE Transactions on Industrial Electronics. 2018, 66(7):5197–5208.

Nagaraju A., Rajender B., A High Gain Single Switch DC-DC Converter with Double Voltage Booster Switched Inductors. Adv. in Sci. Technol. Res. J.; 2023, 17(2),1–11.

Nagaraju A.; Rajender B., A Transformer Less High Gain Multi Stage Boost Converter Fed H-Bridge Inverter for Photovoltaic Application with Low Component Count. J. Eng. Sci. Technol, 2023, 18(2), pp. 1038-1054.

Padmavathi P, Natarajan S. Single switch quasi-Z-source based high voltage gain DC-DC converter. Int. Trans. Electr. Energy Syst.; 2020, 30.

Penghui Ma, W. Liang, H. Chen, Y. Zhang, and X. Hu, "Interleaved high step-up boost converter," Journal of Power Electronics, 2019, vol. 19, pp. 665–675.

Ranganathan S, Arun Noyal Doss M. Formulation and analysis of single switch high gain hybrid DC to DC converter for high power applications. Electronics; 2021, 10(19), 2445.

S. Khan, A. Mahmood, M. Tariq, M. Zaid, I. Khan, and S. Rahman, ``Improved dual switch non-isolated high gain boost converter for DC microgrid application," in Proc. IEEE Texas Power Energy Conf. (TPEC), Feb. 2021, pp. 16,

S. Sadaf, N. Al-Emadi, P. K. Maroti, and A. Iqbal, ``A new high gain active switched network-based boost converter for DC micro-grid application," IEEE Access, 2021, vol. 9, pp. 6825368265, ,

Samadian A, Hosseini SH, Sabahi M, Maalandish M. A new coupled inductor non-isolated high step-up quasi-Z-source DC–DC converter. IEEE Transactions on Industrial Electronics.2019, 67(7):5389–5397.

Saravanan S, Babu NR. Design and development of single switch high step-up DC–DC converter. IEEE J. Emerg. Sel. Top. Power Electron.2018, 6:855–863.

Sarikhani A., Allahverdinejad B. and Hamzeh M., "A Nonisolated Buck–Boost DC–DC Converter with Continuous Input Current for Photovoltaic Applications," in IEEE Journal of Emerging and Selected Topics in Power Electronics, Feb. 2021,vol. 9, no. 1, pp. 804–811.

Sathiya R, Arun Noyal Doss M, ThulasiRaman, NA, Prabhu MM. Non isolated high gain DC-DC converter using sustainable energy. Materials Today Proceedings. Elsevier Journals, 2021, Volume 80, Pages, 2513–2517.

Tole Sutikno, Hendril Satrian Purnama, Nuryono Satya Widodo, Sanjeevikumar Padmanaban, Mohd Rodhi Sahid, A review on non-isolated low-power DC–DC converter topologies with high output gain for solar photovoltaic system applications, *Clean Energy*, Volume 6, Issue 4, 2022, Pages 557–572,

Van Tan Nguyen; Huu Hieu Nguyen; Kim Hung Le; and The Khanh Truong. Expansion of Renewable Energy Capacities in Microgrids Using Robust Control Approaches. GMSARN International Journal,2022, vol. 16, pp. 336-344.

X. Hu, Y. Zhang, X. Liu, Z. Yu, T. He, and L. Mao, "A non-isolated step-up DC-AC converter with reduced leakage current for grid-connected photovoltaic systems," IEEE Access, 2020, Vol. 8, pp. 71907–71916.

Yuttana Kongjeen; Weerayut Eiampong; Krittidet Buayai2; and Kaan Kerdchuen. Voltage Stability Analysis in Microgrids System with Photovoltaic Solar Energy under Uncertainty of Loads Variation. GMSARN International Journal, 2023, 17 . pp. 156-162